JOURNAL OF APPLIED ELECTROCHEMISTRY 14 (1984) 437–448

Impedance of a porous electrode with an axial gradient of concentration

MICHEL KEDDAM. CHRISTIANE RAKOTOMAVO, HISASI TAKENOUTI

Groupe de Recherche No. 4 du CNRS 'Physique des Liquides et Electrochimie', associé à l'Université P. & M. Curie, 4 place Jussieu, 75230 Paris Cedex 05, France

Received 11 September 1983

When the impedance is measured on a battery, an inductive impedance is often observed in a high frequency range. This inductance is frequently related to the cell geometry and electrical leads. However, certain authors claimed that this inductance is due to the concentration distribution of reacting species through the pores of battery electrodes. Their argument is based on a paper in which a fundamental error was committed. Hence, the impedance is re-calculated on the basis of the same principle. The model shows that though the diffusion process plays an outstanding role, the overall reaction rate is never completely limited by this process. The faradaic impedance due to the concentration distribution is capacitive. Therefore, the inductive impedance observed on battery systems cannot be, by any means, attributed to the concentration distribution inside the pores. Little frequency distribution is found and the impedance is close to a semi-circle. Therefore depressed impedance diagrams in porous electrodes without forced convection cannot be ascribed to either a Warburg nor a Warburg–de Levie behaviour.

Nomenclature

A	$D\lvert\Delta C\rvert$ (mole cm s^{-1})
B	$j\omega + K\lvert\Delta C\rvert$ (mole cm s^{-1})
b	Tafel coefficient (V^{-1})
$C(x)$	Concentration of S in a pore at depth x (mole cm^{-3})
C_0	Concentration of S in the solution bulk (mole cm^{-3})
ΔC	$C(x)$ change under a voltage perturbation (mole cm^{-3})
$\lvert\Delta C\rvert$	Amplitude of ΔC (mole cm^{-3})
D	Diffusion coefficient ($cm^2\ s^{-1}$)
E	Electrode potential (V)
ΔE	Small perturbation in E namely a sine-wave signal (V)
$\lvert\Delta E\rvert$	Amplitude of ΔE (V)
F	Faraday constant (96500 A s mol^{-1})
$F(x)$	Space separate variable for C
f	Frequency in Hz (s^{-1})
$g(x)$	$K'C(x)\lvert\Delta E\rvert$ (mole cm s^{-1})
I	Apparent current density (A cm^{-2})
I_{st}	Steady-state current per unit surface of pore aperture (A cm^{-2})
j	Imaginary unit $[(-1)^{1/2}]$
K	Pseudo-homogeneous rate constant (s^{-1})
K'	Potential derivative of K, dK/dE ($s^{-1}\ V^{-1}$)
K^*	Heterogeneous reaction rate constant (cm s^{-1})
L	Pore depth (cm)
n	Reaction order
P	Reaction product
p	Parameter for $F(x)$, see Equation 13
q	Parameter for $F(x)$, see Equation 13
R_e	Electrolyte resistance (ohm cm)
R_p	Polarization resistance per unit surface of pore aperture (ohm cm^2)
R_t	Charge transfer resistance per unit surface of pore aperture (ohm cm^2)
S	Reacting species
S_a	Total surface of pore apertures (cm^2)
S_0	Geometrical surface area
S_p	Developed surface area of porous electrode per unit volume ($cm^2\ cm^{-3}$)
s	Concentration gradient (mole $cm^{-3}\ cm^{-1}$)

0021–891X/84 $03.00 + .12

t	Time	δ	Thickness of Nernst diffusion layer
U	Ohmic drop	λ	Penetration depth of reacting species (cm)
x	Distance from pore aperture (cm)	μ	Penetration depth of a.c. signal determined by the potential distribution (cm)
Z	Faradaic impedance per unit surface of pore aperture (ohm cm^2)	ρ	Electrolyte (solution) resistivity (ohm cm)
Z_x	Local impedance per unit pore length (ohm cm^3)	Φ_0	Flow of S at the pore aperture (mole cm^2 s^{-1})
z	Charge transfer number	ω	Angular freqeuncy of a.c. signal, $2\pi f$ (s^{-1})
α	Porosity	Γ	Integration constant

1. Introduction

In many cases, the impedance of battery systems exhibits an inductive behaviour at relatively high frequencies [1–8]. This inductance is often attributed to the battery cell geometry, electrical leads and connectors [1–3, 5]. Gutman [4], however, linked this phenomenon to a viscoelastic property of the electrolyte. But the frequency range at which the inductance is observed depends on the magnitude of the impedance and hence on the battery capacity [9]. Furthermore, on a flat electrode immersed in the same battery electrolyte, for instance Pb in 5M H_2SO_4, no inductance is observed. These experimental observations are in favour of the geometrical origin of the self-inductance. At least, the inductance observed can hardly be related to physical properties of the electrolyte itself.

Sathyanarayana *et al.* [6] claimed that the inductance observed on a Ni–Cd battery is due to the ferromagnetism of Ni, whereas on a Pb–H_2SO_4 battery, the same phenomenon is attributed to the porous texture of the electrode without any detailed explanation [7]. The impedance of a porous electrode was studied by de Levie [10] on the basis of a model describing the potential distribution in the pore. He showed that if an inductance were observed in a porous electrode, the interfacial impedance on a flat electrode should also be inductive. Thus, according to this study, the porous structure alone cannot give rise to an inductive impedance.

Hampson *et al.* [8, 11–13] repeatedly attributed the origin of this inductive behaviour to the occurrence of reactions within pores on the basis of two theoretical papers by Darby [14, 15]. The latter calculated the Faradaic impedance of a porous gas-diffusion electrode. Unfortunately, the derivation given by Darby is basically incorrect and the inductive impedance may have been mistakenly interpreted in terms of the porous electrode. Based on the same hypotheses used by Darby, the calculation was remade [16].

Initially a first order reaction in a finite pore length is considered. Then the case of semi-infinite pore length is examined as a particular case of the model. An nth order interfacial reaction is analysed. Finally, the applicability of the model to the impedance of battery electrodes is briefly discussed.

2. The model

2.1. *First order reaction and finite pore depth*

The model elaborated by Darby [14] dealt with a concentration distribution in a porous gas-diffusion electrode. However, the concentration of reacting species at the gas–liquid interface is determined by an equilibrium law. The diffusion of reacting species in the gaseous phase is much faster than in the liquid phase and no charge transfer takes place at the gas–electrode interface. Consequently, the reaction rate and the electrode impedance are completely determined by the diffusion in the liquid phase. The model reduces therefore to the simple situation examined below. It is assumed that an electrochemical process:

$$S \rightarrow P + ze^-$$

takes place on the walls of the porous electrode. S is a reaction species, z is the number of elementary charges transferred in this reaction and P is a reaction product. When the reaction progresses, the concentration $C(x)$ of S inside pores damps down as a function of x, the distance from the pore aperture. L is the thickness of the porous electrode ($0 \leqslant x \leqslant L$).

In the presence of a supporting electrolyte, Fick's Second law allows the expression of the one-dimensional concentration profile

$$\frac{\partial C}{\partial t} = D\frac{\partial^2 C}{\partial x^2} - KC \tag{1}$$

where D is the diffusion coefficient and K can be regarded as a pseudo-homogeneous rate constant accounting for the consumption of S on the pore walls. K is to be linked to the heterogeneous electrochemical rate constant K^* by

$$K = S_p K^* \tag{2}$$

where S_p is the developed surface area of the porous electrode per unit volume. Since an electrochemical process is considered, K^* and hence K are both potential dependent. Two boundary conditions should be introduced with Equation 1.

At $x = 0$, $C(x) = C_0$ the concentration in the solution bulk; at $x = L$, $dC(x)/dx = 0$. It may be worth emphasizing that the concentration distribution is axial, that is, perpendicular to the porous electrode surface, and no radial distribution perpendicular to the electrode wall inside the pore is considered. This contrasts with the application of the model developed by de Levie [10] to a Warburg impedance, in which case the concentration distribution is supposed to be radial whereas the potential distribution is axial. Neglecting ohmic effects and the radial gradient of concentration with respect to the axial one, the model can be considered as relevant to a narrow pore in the absence of forced convection and flooded with a highly conductive electrolyte [17].

2.1.1. Steady-state flow. At the steady-state, that is, once the concentration profile is established, $C(x)$ depends no longer on time. Thus, the left-hand term of Equation 1 is equal to zero. This allows calculation of the concentration profile as a function of x.

$$C(x) = C_0 \frac{\cosh\left[(x-L)(K/D)^{1/2}\right]}{\cosh\left[L(K/D)^{1/2}\right]} \tag{3}$$

The flow of S at the pore aperture is equal to the overall rate of consumption of S inside the pores at steady-state and can be derived from the concentration gradient at $x = 0$, hence

$$\begin{aligned} \Phi_0 &= -D\left(\frac{\partial C}{\partial x}\right)_{x=0} \\ &= C_0 (KD)^{1/2} \tanh\left[L(K/D)^{1/2}\right] \end{aligned} \tag{4}$$

The overall consumption of S inside the pores can be equally calculated by integrating the reaction rate on the pore wall from aperture to bottom as follows:

$$\begin{aligned} \Phi_0 &= \int_0^L KC(x)\,dx \\ &= \frac{KC_0}{\cosh\left[L(K/D)^{1/2}\right]} \int_0^L \cosh\left[(x-L)(K/D)^{1/2}\right] dx \\ &= C_0 (KD)^{1/2} \tanh\left[L(K/D)^{1/2}\right] \end{aligned} \tag{5}$$

It can be verified that Equations 4 and 5 yield the same results. The steady-state current per unit surface of pore aperture can be then calculated using Faraday's Law:

$$I_{st} = zF\Phi_0 = zFC_0(KD)^{1/2}\tanh[L(K/D)^{1/2}] \tag{6}$$

2.1.2 Faradaic impedance. As was shown above, at steady-state, the consumption of S inside the pores is equal to the flow of this species at the pore aperture. However, this is no longer valid at non-steady-state, since the concentration of reacting species is time and space dependent inside the pores following Fick's Second law. Darby's derivation (Equation 17 in [14]) was incorrect on this point and misleadingly used Equation 4 for the calculation of the Faradaic impedance. In fact, this procedure is correct for a potential distribution problem [10] provided a quasi-stationary situation is considered in the sense of Maxwell's equations. It would, however, be recalled that Darby's work was a pioneering one in the calculation of Faradaic impedance of porous electrodes and hence at that time the problem was poorly defined. Other hypotheses used in the model remain perfectly valid and are used in this paper.

In order to determine the electrode impedance, the system under investigation is submitted to a small perturbing signal around its steady-state. The response can be derived from the Taylor expansion of Equation 1 limited to first order terms:

$$\frac{d\Delta C}{dt} = D\frac{\partial^2\Delta C}{\partial x^2} - K\Delta C - K'C(x)\Delta E \tag{7}$$

where $K' = dK/dE$. If a sine wave voltage perturbation is used:

$$\Delta E = |\Delta E|\exp(j\omega t) \tag{8}$$

where $|\Delta E|$ is the amplitude of the a.c. signal and ω is its angular frequency. The concentration change also follows a sine wave modulation provided that $|\Delta E|$ is small enough, i.e. the system deviation remains in the linear domain. Equation 7 can be rewritten as:

$$j\omega\Delta C = D\frac{\partial^2\Delta C}{\partial x^2} - K\Delta C - K'C(x)\Delta E \tag{9}$$

Solutions of Equation 9 are of the form:

$$\Delta C = |\Delta C|\exp(j\omega t)F(x) \tag{10}$$

Combining Equations 8–10 yields:

$$(K + j\omega)|\Delta C|F(x) = D|\Delta C|\frac{\partial^2 F(x)}{\partial x^2} - K'C(x)|\Delta E| \tag{11}$$

Equation 11 can be expressed by:

$$AF''(x) - BF(x) = g(x) \tag{12}$$

where

$$A = D|\Delta C|$$

$$B = (K + j\omega)|\Delta C|$$

$$g(x) = K'C(x)|\Delta E|$$

The general form of the solution to Equation 12 when $g(x) = 0$ is:

$$F(x) = p\exp\left[-x\left(\frac{B}{A}\right)^{1/2}\right] + q\exp\left[x\left(\frac{B}{A}\right)^{1/2}\right] \tag{13}$$

A particular solution of the complete equation is expressed by:

$$F_0(x) = \frac{C(x)K'|\Delta E|}{AK/D - B} = -\frac{K'C(x)}{j\omega}\frac{|\Delta E|}{|\Delta C|} \tag{14}$$

Then the general solution can be written as:

$$F(x) = p \exp\left[-\alpha\left(\frac{B}{A}\right)^{1/2}\right] + q \exp\left[\alpha\left(\frac{B}{A}\right)^{1/2}\right] - \frac{K'C(x)}{j\omega}\frac{|\Delta E|}{|\Delta C|} \tag{15}$$

The boundary condition for $x = 0$ gives:

$$\Delta C = 0 \text{ at } x = 0 \text{ hence } \quad p + q - \frac{C_0 K' |\Delta E|}{j\omega |\Delta C|} = 0 \tag{16}$$

and

$$d\Delta C/dx = 0 \text{ at } x = L \text{ gives } \quad \frac{p}{q} = \exp\left[2L\left(\frac{B}{A}\right)^{1/2}\right] \tag{17}$$

Equations 16, 17 allow the calculation of p and q and yield:

$$F(x) = \frac{K'C_0|\Delta E|}{j\omega|\Delta C|}\left[\frac{\cosh(x-L)(B/A)^{1/2}}{\cosh L(B/A)^{1/2}} - \frac{\cosh(x-L)(K/D)^{1/2}}{\cosh L(K/D)^{1/2}}\right] \tag{18}$$

At the abscissa x, the local impedance, Z_x, per unit pore length and per unit surface of pure aperture is

$$\frac{1}{Z_x} = zF\frac{\Delta(KC)}{\Delta E} = zF\left(K'C(x) + KF(x)\frac{|\Delta C|}{|\Delta E|}\right) \tag{19}$$

The total impedance is calculated by summing the local contribution of Z_x over the whole pore length:

$$\frac{1}{zFZ} = \frac{1}{zF}\int_0^L \frac{1}{Z_x}\,dx$$

$$= K'\int_0^L C(x)\,dx + \frac{KK'C_0}{j\omega}\int_0^L\left[\frac{\cosh(x-L)(B/A)^{1/2}}{\cosh L(B/A)^{1/2}} - \frac{\cosh(x-L)(K/D)^{1/2}}{\cosh L(K/D)^{1/2}}\right]dx \tag{20}$$

and finally for the impedance of the pore:

$$\frac{1}{zFZ} = K'C_0(D/K)^{1/2}\tanh L(K/D)^{1/2} + \frac{KK'C_0}{j\omega}[(A/B)^{1/2}\tanh(B/A)^{1/2} - (D/K)^{1/2}\tanh(K/D)^{1/2}] \tag{21}$$

The particular case of a semi-infinite pore length can be easily examined by setting $L \to \infty$ in Equation 21. One has for the limiting value Z_∞ of the impedance:

$$\frac{1}{zFZ_\infty} = K'C_0(D/K)^{1/2} + \frac{KK'C_0}{j\omega}[(A/B)^{1/2} - (D/K)^{1/2}] \tag{22}$$

Limiting cases as $\omega \to 0$ and $\omega \to \infty$ are of interest for predicting the size of the impedance diagram. For a semi-infinite pore length the low frequency limit of the impedance (polarization resistance R_p) is twice as great as the high frequency limit (charge transfer resistance R_t).

$$R_p = 2R_t. \tag{23}$$

This relation holds whatever the kinetic law of the electrochemical process $K(E)$. This result is clearly the impedance counterpart of the doubling of the Tafel slope under ohmic or diffusion control established by Austin and Lerner [17].

In the case of a finite pore length it can be shown analytically [16] that $R_p < 2R_t$.

2.2. *Case of non-first-order kinetics*

This case was also treated by Darby [15] but the derivation was also incorrect for the same reason as shown above. The electrochemical process can be written as

$$n\mathrm{S} \to \mathrm{P} + ze^-$$

The concentration profile at steady state is:

$$D\frac{d^2C}{dx^2} = KC^n \tag{24}$$

Integration of Equation 24 is performed by setting $dC/dx = s$

$$\frac{d^2C}{dx^2} = \frac{ds}{dx} = \frac{ds}{dC}\frac{dC}{dx} \tag{25}$$

A first integration gives:

$$s^2 = \frac{2K}{D}\int C^n dC + \Gamma_1 = \left(\frac{dC}{dx}\right)^2 \tag{26}$$

and a second integration:

$$x + \Gamma_2 = \int \frac{dC}{\Gamma_1 + \left(\frac{2K/DC^{n+1}}{n+1}\right)^{1/2}} \tag{27}$$

Γ_1 and Γ_2 are integration constants.

If Γ_1 is not equal to zero, the equation has, in general, no analytical solution. The case considered by Darby [15] corresponds to $\Gamma_1 = 0$ consistent with C and $dC/dx \to 0$ as $x \to \infty$ (semi infinite pore length). The boundary condition at $x = 0$, $C = C_0$ determines Γ_2 and allows us to obtain:

$$C(x) = C_0\left\{x(n-1)\left[\frac{KC_0^{n-1}}{2D(n+1)}\right]^{1/2} + 1\right\}^{2/(1-n)} \tag{28}$$

The penetration depth can no longer be defined in this nonlinear case. The concentration profile depends on C_0. As recognized by Darby [15] the electrode impedance cannot be calculated analytically. Nevertheless one can evaluate the values of R_t and R_p.

As above, the local impedance Z_x is given by:

$$\frac{1}{zFZ_x} = K'C^n + KnC^{n-1}\frac{|\Delta C|}{|\Delta E|}F(x) \tag{29}$$

$(|\Delta C|/|\Delta E|)F(x)$ tends to zero as $\omega \to \infty$, thus the charge transfer resistance is equal to:

$$\frac{1}{zFR_t} = K'\int_0^\infty C^n dx \tag{30}$$

Substituting C^n from Equation 24, yields:

$$\frac{1}{R_t} = 2zFK'C_0^{3-n/2}\left[\frac{D}{2K(n+1)}\right]^{1/2} \tag{31}$$

The polarization resistance calculated from the steady-state current voltage equation yields:

$$\frac{1}{R_p} = zFK'C_0^{3-n/2}\left[\frac{D}{2K(n+1)}\right]^{1/2} \tag{32}$$

Therefore Equations 31, 32 show that even with a reaction order different from one, $R_p = 2R_t$ is fulfilled for a semi-infinite pore length.

3. Results of numerical simulation

3.1. *Steady-state*

The shape of the complex impedance diagram generated by Equation 21 cannot be established analytically. Therefore numerical simulations were performed. A Tafel law was assumed to control the

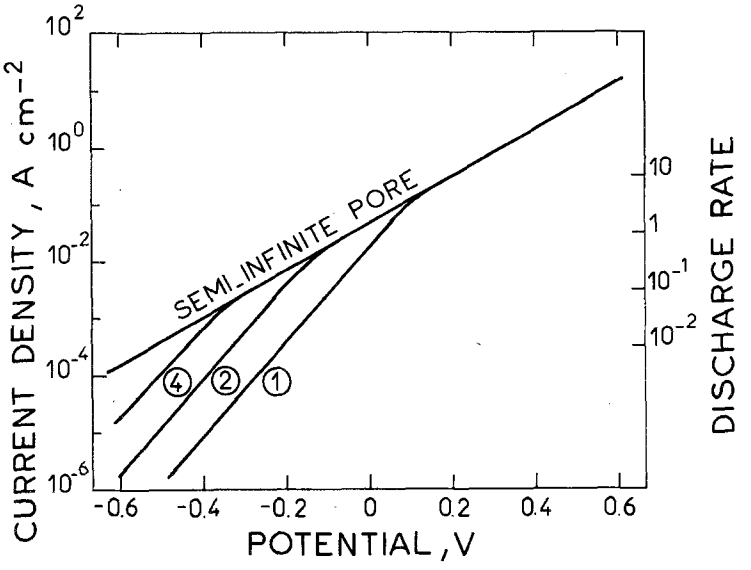

Fig. 1. Polarization curve of porous electrode. The constants used are: $C_0 = 5 \times 10^{-3}$ mol cm^{-3}; $D = 1 \times 10^{-5}$ cm^2 s^{-1}: $z = 1$; $K = 1 \times 10^{-3} \exp(19.2E)$ s^{-1}. The thicknesses of the porous electrodes are: (1) 0.4; (2) 4 and (4) 40 mm. On the right ordinand-axis, the discharge rate for the Pb-battery is shown. The scale is given in the ratio of d.c. current flow over that corresponding to a complete discharge of the battery within 10 h.

potential dependence of the rate constant:

$$K^* = K_0^* \exp(bE) \tag{33}$$

where the Tafel exponent b lies between 0 and 38.4 V^{-1} for $z = 1$.

The pseudo-homogeneous rate constant is deduced according to Equation 2. Fig. 1 depicts the steady-state flow of S for three different values of L: 0.4, 4 and 40 mm. One can distinguish two ranges of electrode kinetics. At low anodic overvoltages (low reaction rate) the Tafel slope has the same value as on a flat electrode chosen for the numerical computation (120 mV decade^{-1}) whereas at high overvoltages (high reaction rate) the Tafel slope is twice as great. This behaviour was first pointed out by Austin and Lerner [17]. The deeper the pore structure, the lower is the potential of transition from the flat electrode regime to the porous one. This classical result is substantiated by the concentration profiles shown in Fig. 2 for $L = 4$ mm at various electrode potentials in a range covering the transition region in Fig. 1, Curve 2. At low overvoltages the diffusion is fast enough to supply the reacting species

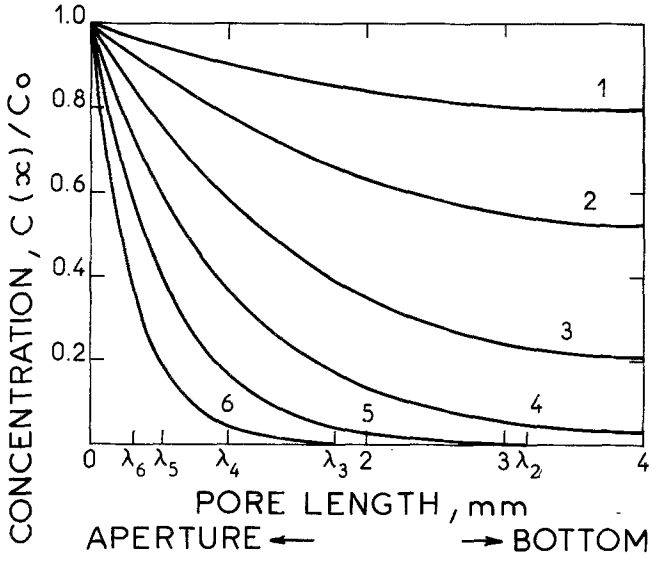

Fig. 2. Reduced concentration profile for different reaction rates for $L = 4$ mm. (1) $E = -0.18$ V, $I_{st} = 5.27$ mA cm^{-2}; (2) $E = -0.12$ V, $I_{st} = 13.0$ mA cm^{-2}; (3) $E = -0.06$ V, $I_{st} = 26.5$ mA cm^{-2}; (4) $E = 0$ V, $I_{st} = 48.2$ mA cm^{-2}; (5) $E = 0.06$ V, $I_{st} = 85.8$ mA cm^{-2} and (6) $E = 0.12$ V, $I_{st} = 153$ mA cm^{-2}. Other constants are shown in Fig. 1.

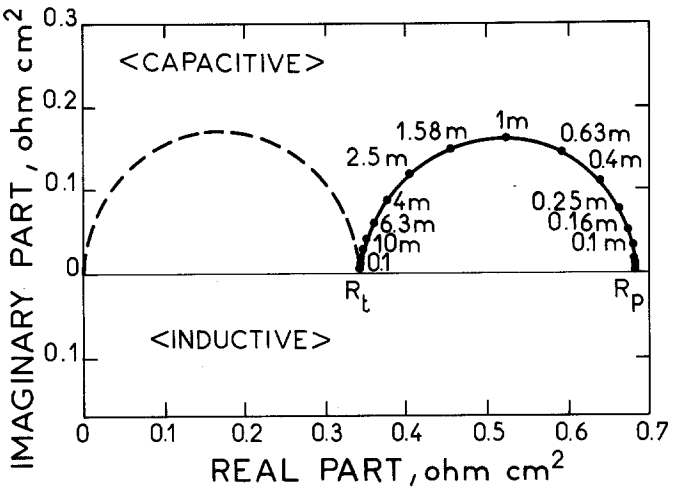

Fig. 3. Impedance diagram for $E = 0.12$ V, other constants are shown on Fig. 1.

up to the bottom of the pore (flat electrode regime). At high overvoltages the electrode behaves like a semi-infinite pore.

Inversely, Fig. 4 shows concentration profiles for various L at a constant potential. In the same figure is also presented the ratio $I_L/I_\infty = \tanh(L/\lambda)$ according to Equation 6 for the ratio of current for the actual pore length I_L to that of the semi-infinite pore I_∞.

3.2. *Impedance*

An impedance diagram calculated for $E = 0.12$ V is shown in Fig. 3. This diagram corresponds to a semi-infinite pore. It can be verified in agreement with analytical prediction that $R_p = 2R_t$. The double layer capacitance in parallel with the charge transfer resistance gives rise to the semi-circle shown as a broken line. A clear separation of the charge transfer and diffusion arcs is ensured by the very small double layer capacitance. Large specific areas of the porous material will lead to a frequency shift towards lower frequencies and to a serious overlapping with the diffusion arc.

The contribution of the axial diffusion appears as a nearly perfect semicircle. This was not obvious

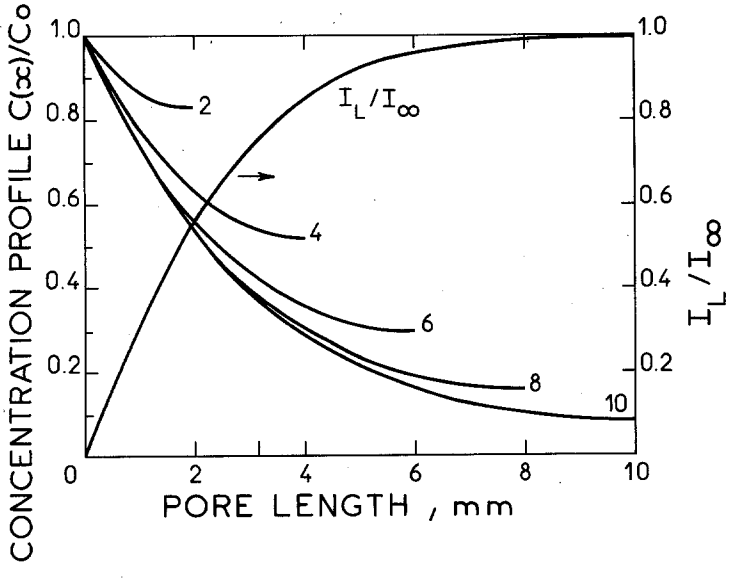

Fig. 4. Reduced concentration profile for different L. The pore thickness is indicated near each curve in mm. I_L/I_∞ indicates the ratio of steady-state current for finite pore length I_L over that of the semi-infinite pore I_∞.

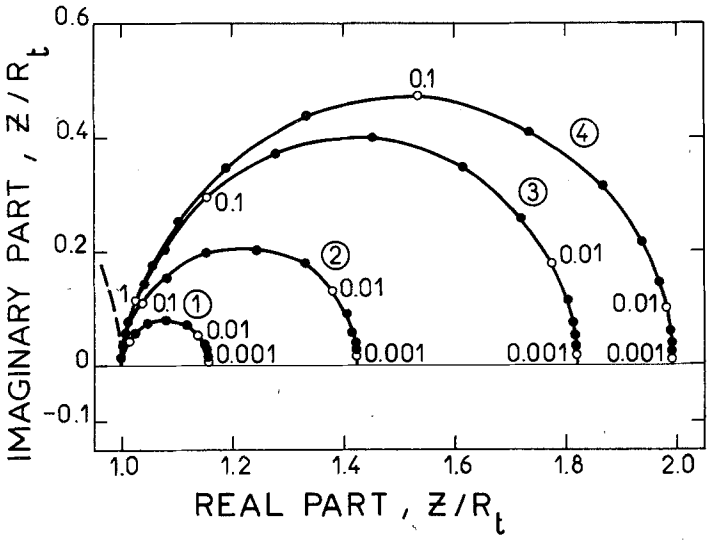

Fig. 5. Reduced impedance diagram showing the low frequency range corresponding to the impedance of the diffusion process. R_t is the charge transfer for each potential (1) $E = -0.18$ V; (2) $E = -0.12$ V; (3) $E = -0.06$ V; (4) $E = 0$ V.

from the analytical expression. It can also be noted that very low frequencies are implied in spite of the relatively high current density (0.15 A cm^{-2}). As can be seen from Equation 21 the time constant for the admittance plane is close to K.

Fig. 5 shows in a reduced form Z/R_t, the change of impedance with respect to reaction rate. The smaller the reaction rate, the smaller is the relative size of the diffusion loop as the electrode behaviour approaches that of a flat electrode. The diffusion loops remain practically similar in shape. This is illustrated in Fig. 6 in the Bode plane ($\log|Z|$, $\log f$) at two different over-voltages, two different impedance scales are used. These plots indicate more clearly the similarity of the diffusion loops and also their frequency shift. For comparison, the impedance of a dummy cell, shown in the insert, is also plotted as a broken line. Only a slight difference is observed between 2×10^{-4} and 5×10^{-3} Hz. Fig. 7 illustrates in a somewhat different way, the result shown in Fig. 5. The variation of the product $R_p I_{st}$ commonly used as a kinetic criterion is of special interest. It shows a very steep transition from the flat electrode regime (52 mV) to the porous semi-infinite regime (104 mV).

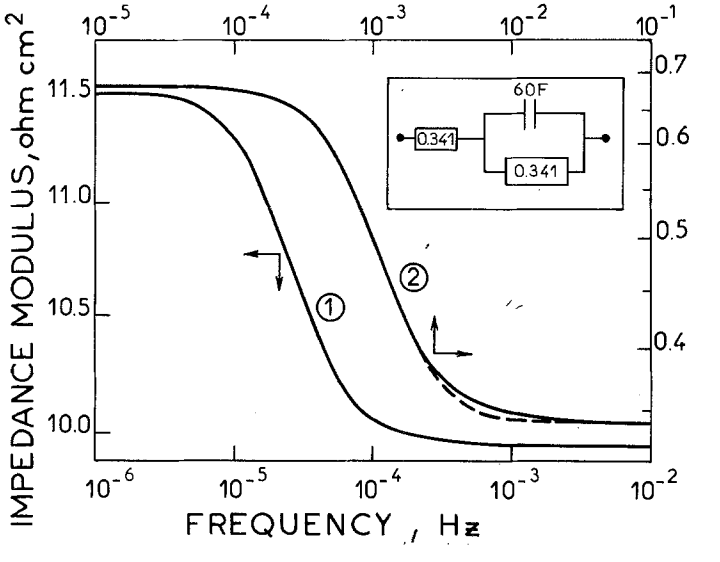

Fig. 6. Bode plot of the electrode impedance. (1) $E = -0.18$ V; (2) $E = 0.12$ V. The insert shows the dummy cell giving the impedance close to Curve 2.

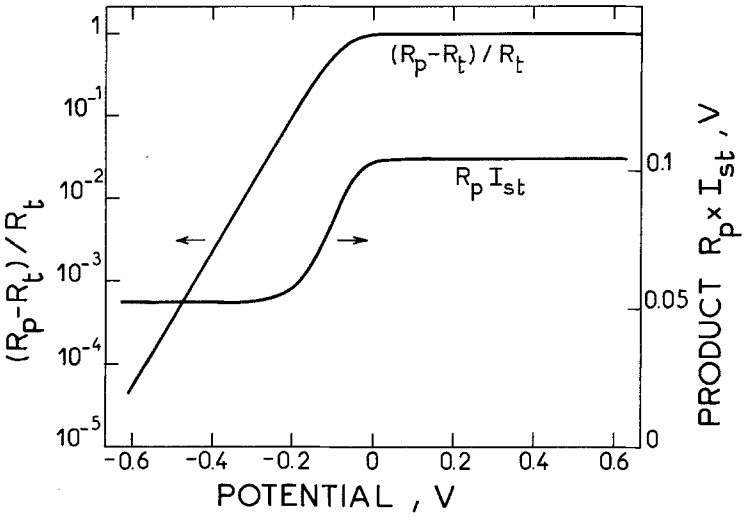

Fig. 7. Relative change of R_p/R_t and $R_p I_{st}$ values. Constants are as for Fig. 1.

4. Discussion in the framework of battery electrodes

A correct derivation of the impedance arising from an axial concentration gradient in a one-dimensional porous structure and with negligible ohmic effect gives no inductance at all. Therefore, the use of this model for interpreting high frequency inductive behaviour observed on many battery electrodes is totally irrelevant.

In agreement with previous studies of this model at steady-state the limitation by diffusion of the overall current through the porous structure is only partial. The polarization resistance is at most twice the charge transfer resistance. As shown in Fig. 4 the frequency range covered by the diffusion dependent part of the impedance is very low (millihertz range). According to Equation 21 this frequency range depends on K. This situation is very similar to the Faradaic impedance related to an homogeneous chemical reaction in the diffusion layer [18]. It contrasts with the usual diffusion impedance on a flat electrode for which the characteristic frequency is fixed by δ^2/D, δ being the thickness of the Nernst diffusion layer. In the case of an impedance tied to a heterogeneous reaction on a flat electrode the relaxation frequency is linked to the reaction rate.

The validity of the assumptions regarding the predominance of the axial gradient and the negligible effect of ohmic drop can be assessed in the case of an actual Pb–H_2SO_4 battery. Bode [19] indicated that lead sulphate precipitation is limited to the vicinity of the porous electrode surface at high discharge rate. The penetration depth was estimated to be 0.2 mm at a discharge current density of 180 mA cm^{-2}. If the pore texture is assumed constant over the whole electrode thickness, the current density can be related to the discharge rate as shown in Fig. 1. The total surface of pore aperture S_a can be evaluated with the porosity α and the geometrical surface area S_0:

$$S_a = \alpha S_0 \tag{34}$$

Let the apparent current density be I, then I_{st} can be calculated by:

$$I_{st} = \frac{I}{\alpha} = \frac{zFC_0}{\alpha}(KD)^{1/2} \tag{35}$$

where z stands for the charge transfer number. From Equation 35 one obtains the penetration depth, λ

$$\lambda = \left(\frac{D}{K}\right)^{1/2} = \frac{zC_0FD}{I} \tag{36}$$

By using values of $D = 1 \times 10^{-5}$ cm^2 s^{-1}, $C_0 = 5 \times 10^{-3}$ and $z = 2$, one calculates $\lambda = 0.6$ mm

at $I = 180\,\text{mA cm}^{-2}$. This value is slightly greater than that observed experimentally, but remains in the correct order of magnitude.

The electrolyte resistance, through the porous electrode per unit pore length and per unit geometrical surface can be calculated by:

$$R_e = \rho/\alpha \tag{37}$$

where ρ indicates the electrolyte resistivity. The ohmic drop U under d.c. polarization for the penetration depth λ is thus:

$$U = IR_e\lambda = zC_0FD\rho \simeq 13\,\text{mV} \tag{38}$$

with $\rho = 1.3$ ohm cm whatever the current density. That is, the ohmic drop of the d.c. polarization is negligible.

For the impedance diagram, the penetration depth of the a.c. signal μ should be taken into consideration. Though the actual electrode has an intricate pore texture, the potential distribution can be correctly expressed by an equivalent cylindrical pore model [20, 21]. If the impedance at the developed surface is reduced to that due to the double layer capacitance C_d (at sufficiently high frequency this is usually true), μ can be calculated by [22]:

$$\mu = \frac{1}{2}\left(\frac{r}{\omega\rho C_d}\right)^{1/2} \tag{39}$$

If it is assumed that $r = 0.1\,\mu\text{m}$ and $C_d = 20\,\mu\text{F cm}^{-2}$, one evaluates $\mu = \lambda = 0.2\,\text{mm}$, $f = 0.5\,\text{Hz}$.

In other words the potential distribution may affect the impedance diagram on the rather high frequency side with the respect to the diffusion contribution.

5. Conclusion

The model proposed by Darby [14, 15] of axial diffusion in a cylindrical pore and no ohmic effect cannot be invoked to explain the inductive behaviour of porous electrode. Correctly derived, the impedance linked to this description is consistent with the steady-state treatment. Estimation of the concentration gradient and potential distribution indicates that the model can be representative of the situation in lead acid battery electrodes. Calculation of the impedance of porous structures under mixed control by potential and concentration is presently in progress.

Acknowledgements

C. Rakotomavo thanks the Compagnie Européenne d'Accumulateurs for financial support.

References

[1] E. Willihnganz, *J. Electrochem Soc.* **102** (1965) 99.
[2] J. Euler and K. Dehmelt, *Z. Elektrochem.* **61** (1957) 1200.
[3] J. J. Lander and E. E. Nelson, *J. Electrochem. Soc.* **107** (1960) 722.
[4] F. Gutmann, *ibid.* **112** (1965) 94.
[5] M. Keddam. Z. Stoynov and H. Takenouti, *J. Appl. Electrochem.* 7 (1977) 539.
[6] S. Sathyanarayana, S. Venugopalan and M. L. Gopikanth, *ibid.* 9 (1979) 125.
[7] M. L. Gopikanth and S. Sathyanarayana, *ibid.* 9 (1979) 369.
[8] N. A. Hampson, S. A. G. R. Karunathilaka and R. Leek, *ibid.* **10** (1980) 3.
[9] R. J. Brodd and H. J. Dewane, *J. Electrochem. Soc.* **110** (1963) 1091.
[10] R. de Levie, 'Advances in Electrochemistry and Electrochemical Engineering', edited by P. Delahay, Vol. 6, John Wiley and Sons, New York (1967) p. 329.
[11] N. A. Hampson and S. Kelly, *J. Appl. Electrochem* **11** (1981) 751.
[12] C. Lazarides and N. A. Hampson, *Surf. Technol.* **16** (1982) 255.
[13] *Idem, ibid.* **17** (1982) 205.
[14] R. Darby, *J. Electrochem. Soc.* **113** (1966) 392.
[15] *Idem, ibid.* **113**, (1966) 496.

[16] C. Rakotomavo, Dissertation thesis, Paris (1983).
[17] L. G. Austin and H. Lerner, *Electrochim. Acta* 9 (1964) 1469.
[18] K. J. Vetter, Electrochemical Kinetics', Springer Education (1961).
[19] H. Bode, 'Lead–acid batteries', translated by R. J. Brodd and K. V. Kordesch, John Wiley and Sons, New York (1977).
[20] J. P. Candy, P. Fouilloux, M. Keddam and H. Takenouti, *Electrochim. Acta* **26** (1981) 1029.
[21] J. P. Candy, P. Fouilloux, M. Keddam and H. Takenouti, *ibid.* **27** (1982) 1585.
[22] H. Keiser, K. D. Beccu and M. A. Gutjahr, *ibid.* **21** (1976) 539.